A temporal and morphological framework for flower development in *Antirrhinum majus*

Coral A. Vincent and Enrico S. Coen

Abstract: The entire course of flower development in *Antirrhinum majus* L., from initiation to maturity, is described in terms of regular time intervals. Floral meristem and bud morphology was determined by scanning electron microscopy for a sequence of 58 plastochrons. These can be grouped to define 15 stages or 7 phases of development, providing a temporal framework for gene expression and key morphological events, such as the formation of the complex corolla. The time course is also used to estimate overall growth rates of sepals and petals. Sepals initially grow at a constant rate, but growth rate gradually declines at later stages and sepal growth eventually arrests before flower development is complete. Petals initially grow at a similar rate to that of early sepals, but this growth rate is maintained for a longer period, accounting for the larger size of mature petals relative to sepals. Comparisons with *Arabidopsis* indicate that the duration of growth also makes an important contribution to variation in flower size.

Key words: Antirrhinum, flower development, meristems, zygomorphy, developmental timing, petal.

Résumé : Les auteurs décrivent l'ensemble de la chronologie du développement floral chez l'*Anthirrhinum majus* L., de l'initiation à la maturité, en termes d'intervalles réguliers. Ils ont observé le méristème floral et la morphologie du bourgeon, en microscopie électronique par balayage, au cours d'une séquence de 58 plastochrons. On peut les regrouper pour définir 15 stades et 7 phases de développement, fournissant un cadre temporel pour l'expression des gènes et des évènements morphologiques déterminants, tels que la formation de la corolle complexe. On utilise également la chronoséquence pour évaluer les taux globaux de croissance des sépales et des pétales. Au début, les sépales poussent à vitesse constante, mais le taux de croissance diminue graduellement vers les derniers stades et la croissance des sépales s'arrête éventuellement, avant que le développement floral soit complet. Au début, les pétales poussent à un rythme similaire à celui des sépales au départ, mais cette croissance se maintient pendant une plus longue période, ce qui explique la plus grande dimension des pétales par rapport aux sépales. Des comparaisons avec l'*Arabidopsis* indiquent que la durée de la croissance apporte également une importante contribution à la variation de la dimension des fleurs.

Mots clés : Antirrhinum, développement floral, méristèmes, zygomorphie, chronologie du développement, pétale.

[Traduit par la Rédaction]

Introduction

The molecular genetic control of flower development has been extensively studied in several model species, most notably in *Arabidopsis thaliana* (L.) Heynh. and *Antirrhinum majus* L. (Lohman and Weigel 2002). These studies have largely concentrated on early developmental stages when the number, identity, and asymmetry of floral organs are first established. However, many key floral features, such as organ shape and size, arise at later stages of development. Moreover, variation in these features provides much of the diversity in floral form. For example, species in the Scrophulariaceae, the family to which *Antirrhinum* belongs, show great diversity in corolla shape (Kampny 1995; Reeves and Olmstead 1998; Endress 1998; Canne-Hilliker 1987). Studying the processes that underlie these forms requires a temporal and morphological framework for the whole of floral development, from initiation to maturity. A framework of this kind has been previously described for *Arabidopsis* (Smyth et al. 1990) and for early stages of *Antirrhinum* development (Carpenter et al. 1995; Awasthi et al. 1984; Singh and Jain 1979). Here we extend the framework for *Antirrhinum* to cover the whole of flower development, including formation of its complex corolla.

Several approaches may be used to describe the sequence of events during morphogenesis. One is to divide development into stages based on morphological landmarks. This was employed for *Arabidopsis* (Smyth et al. 1990), and although it has the advantage of allowing stages to be readily assigned, it does not directly convey the timing of events. Alternatively, development can be subdivided according to regular time intervals upon which morphological landmarks are then mapped. In plants this can be most naturally done using plastochron number or index, which reflects time if plastochron number is constant throughout development (Erickson and Michelini 1957). We adopt this approach here, as it provides a strict temporal framework for mapping developmental events and growth patterns (Ritterbusch 1990*a*, 1990*b*; Ritterbusch and Wunderlin 1989).

Received 30 September 2003. Published on the NRC Research Press Web site at http://canjbot.nrc.ca on 4 June 2004.

C.A. Vincent[1] and E.S. Coen.[2] John Innes Centre, Colney Lane, Norwich, NR4 7UH, England.

[1]Present address: Max-Planck-Institut für Züchtungsforschung, Carl-von-Linné-Weg 10, 50829 Köln, Germany.
[2]Corresponding author (e-mail: Enrico.Coen@bbsrc.ac.uk).

 doi: 10.1139/B04-042

Applying the plastochron as a temporal measure to the whole of flower development, from initiation to maturity, presents two problems. First, because the floral plastochron can be quite small relative to the entire span of floral development, the number of plastochrons that need to be covered can be large (e.g., 250 in the case of foxglove (*Digitalis purpurea*), Ritterbusch 1990*a*). Secondly, many indeterminate inflorescences, such as those of *Antirrhinum*, eventually "peter out" and cease producing flowers, so the plastochron cannot be assumed to be constant at late stages. This means that it may not be possible to get the entire developmental series reflecting constant plastochrons from a single inflorescence. We addressed these issues by restricting our developmental analysis to only the first 15 flowers of the inflorescence. By analysing this region on synchronized plants we show that it is possible to cover the entire span of floral development in terms of regular plastochrons.

Materials and methods

The floral stages of *A. majus* development were determined by analysing stock JI2, which carries the pal^{rec-2} flower pigment mutation (Carpenter et al. 1987). After germination, the plants were grown for about 5 weeks under noninductive conditions (8 h light : 16 h dark) at 25 °C. About 30 plants of a similar size and leaf number (e.g., 16 visible leaves) were selected for the experiment. This synchronized population was induced to flower simultaneously by increasing the day length to 16 h (inductive conditions). Plants were then harvested at 4-d intervals (equivalent to ~10 plastochrons) and the lowest 15 flowers analysed.

Scanning electron microscopy was carried out on plastic replicas of flowers and developing meristems or on material that was critical point dried. The plastic replicas were prepared as described in Green and Linstead (1990). Material for critical point drying was first fixed in 2.5% (*m*/*v*) glutaraldehyde in 0.002 mol/L phosphate buffer (pH 7) containing 0.01% (*v*/*v*) Nonidet P-40 at 4 °C for at least 12 h. They were then rinsed in phosphate buffer before dehydration through an ethanol series. Samples were then critical point dried using CO_2.

Sepal and petal areas were calculated for the dorsal sepal and right dorsal petal. The organs were dissected and flattened out between two glass plates and then scanned into a computer. Their outline was traced by hand and the area therein calculated using a customized program written in MATLAB. Data were collected from two independent experiments for the first 15 flowers from each of three plants at 4, 8, 12, 16, 20, 24, and 28 d after floral induction and aligned to give continuous growth curves.

Results

Wild-type inflorescences of *Antirrhinum* are indeterminate racemes with spiral phylotaxis. To ensure that stages being compared were separated by a similar plastochron, only the first 15 plastochrons from synchronized plants were analysed. By comparing plants harvested at different times, meristems that had been initiated at the same time and under the same conditions, but had reached different development stages, could be analysed. The full range of flower development could be covered by overlapping the data obtained.

It took about 24 d from induction to the opening of the first flower (Fig. 1). Plastochron for the first 15 flowers was estimated by several methods: comparing the number of floral meristems on plants harvested at different early time points, observing the extent of overlap in development between later time points, and recording floral emergence times. All methods gave similar plastochron values of about 10 h for each of the first 15 flowers. Therefore, if the apical meristem had continued initiating nodes at this rate, the inflorescence (raceme) would have contained about 58 nodes (i.e., the number of 10-h intervals in 24 d) from bract initiation to the fully opened flower. Each flower and subtending bract was staged according to the number of plastochrons that separated it from the youngest meristem at the apex (P0). A fully mature flower corresponded to P57. The first 18 plastochrons (P0–P17) cover five previously defined morphological stages 0–4 (Table 1). These stages were defined according to morphology and therefore do not have the same duration (average stage duration = 18/5 = 3.6 plastochrons). To provide a more direct relationship between staging and developmental time, the stages after stage 4 were assigned according to regular time intervals. A time interval of 4 plastochrons was convenient, as this is similar to the average duration of the previously defined stages 0–4. This gave a total of 15 stages (Table 1, Fig. 2). Morphology was then mapped onto the various stages. Stages 0–4 have been previously described by Carpenter et al. (1995) and will only be briefly mentioned here. To provide a coarser temporal staging of development, the 15 stages were grouped into 7 phases, each lasting around 8 plastochrons (Table 1).

Phases of development

Phase A (stages 0–1)

At stage 0, the bract primordium comprised a small group of cells and was visible as a bulge on the periphery of the inflorescence apex (Fig. 2). As the primordium grew outwards, it became separated from the inflorescence apex by a crease and started to arch over the apex (Fig. 2, P0–P5). The beginning of stage 1 was marked by the appearance of a floral meristem (Fig. 2, f) in the axil of the bract primordium (Fig. 2, P6). The floral meristem comprised a small elliptical group of cells lying between a crease at the base of the bract and the apical meristem (Fig. 2, P6–P7). By the end of stage 1, the bract primordium completely covered and protected the eye-shaped floral meristem (note that the bract has been removed from P7 in Fig. 2).

Phase B (stages 2–4)

At stage 2, the floral meristem was raised like a loaf of bread (Fig. 2). By stage 3, the floral meristem had assumed a more pentagonal shape as the five-fold symmetry of the flower started to become evident (Carpenter et al. 1995). By stage 4, sepal primordia were visible (the most dorsal sepal primordium was narrower and shorter than the other four sepal primordia, indicating that its growth was slightly retarded or that it was initiated slightly after the other four sepals). As the five sepal primordia grew around the periphery of the bud, a crease formed at the junction between each sepal primordium and the central meristematic dome, giving

Fig. 1. Stages and phases of *Antirrhinum* flower development. Under the growth conditions employed here it takes about 24 d from bract initiation (P0) to a fully mature open flower, corresponding to 58 plastochrons of 10 h each. These plastochrons have been standardized and grouped into 15 stages (0–14). From stage 4 onwards, each stage lasts 4 plastochrons, or approximately 40 h. These 15 stages have been further grouped into 7 phases, each phase lasting approximately 80 h (3.5 d).

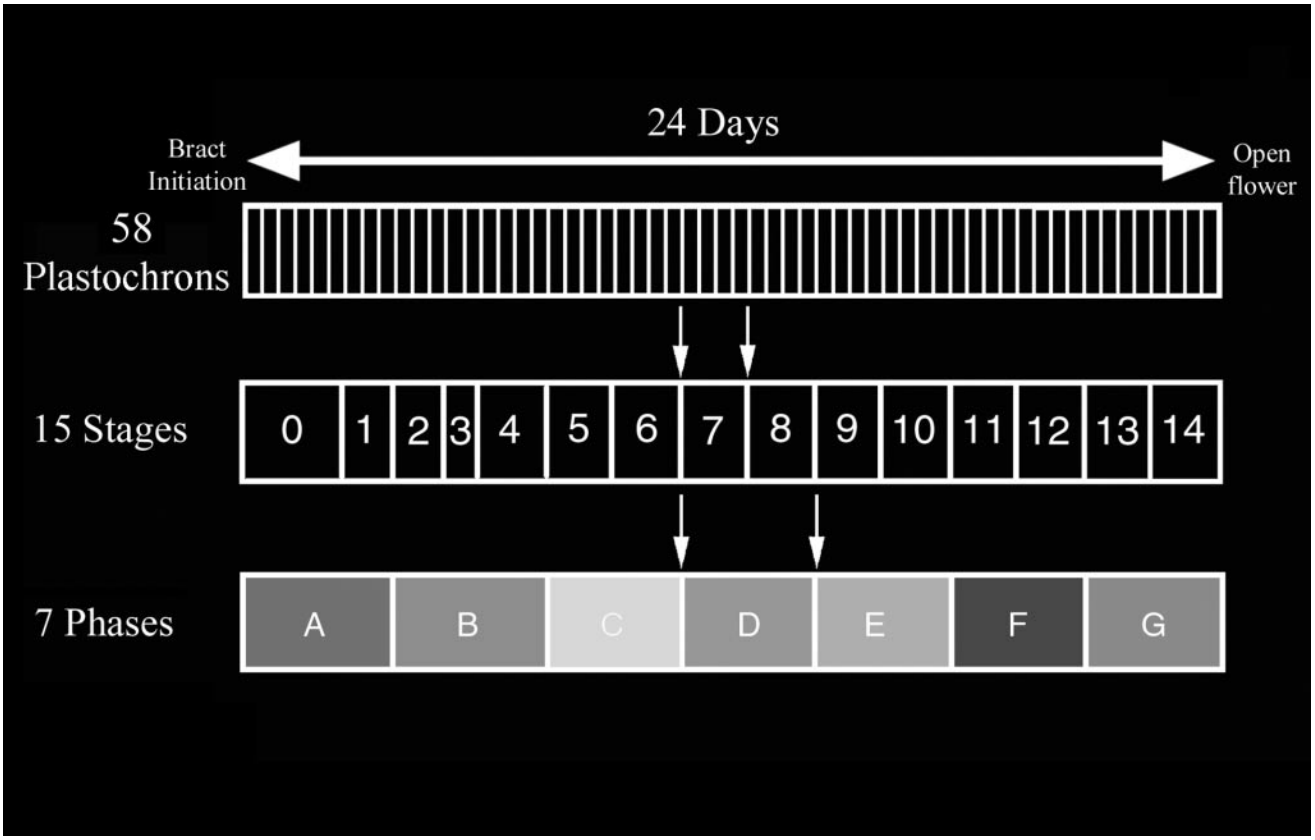

a pentagonal boundary to the dome (Fig. 2). By the end of phase B, the floral bud exhibited its characteristic bilateral symmetry, and the pentamerous calyx of the first whorl was clearly visible.

Phase C (stages 5–6)

Stage 5 began when the five petal primordia of whorl 2 became visible as small oval mounds at each vertex of the pentagonal central dome (Fig. 2). The sepal primordia overlapped each other, covering the bud (note that the sepals have been removed from this stage onwards in Fig. 2). Stamen primordia, which may have initiated at the same time or slightly after the petal primordia, were also visible in whorl 3 as four round mounds, two in ventral and two in lateral positions (Fig. 2), alternate with the petal primordia. Towards the end of stage 5, the fifth stamen (staminode) primordium also became visible in the dorsal position.

At stage 6, the corolla tube became visible as the region where the petals were united at their base. The five corolla lobes partially covered the ventral and lateral stamens, which arched inwards and had curved tips. The staminode was retarded in growth relative to the other stamens. The carpel primordia first appeared at the start of stage 6, creating a central cleft along the dorsoventral axis, slightly offset towards the dorsal side by the ventral stamens (Fig. 2). This cleft deepened at the dorsal and ventral poles as two crescent-shaped carpel primordia widened and elongated. Thus, by the end of phase C, all the primordia of the flower had emerged.

Phase D (stages 7–8)

The corolla almost covered the stamens in stage 7. This stage began when swellings (microsporangia) could be observed on the abaxial side of the ventral and lateral stamens. The development of the dorsal staminode appeared to have arrested.

At stage 8, the corolla lobes completely covered the inner whorls of the bud and began to overlap each other (Fig. 2). Trichomes were first visible on the abaxial surface around the base of the corolla tube (arrow, Fig. 2, stage 8), followed a few plastochrons later by the appearance of hairs cells on the adaxial surface at the junctions between lateral and ventral petals. In whorl 3, the basic external structure of the stamens was established: the two bilocular anther sacs and rudimentary filament could all be seen (Fig. 3). The top surfaces of the developing style came together during stage 8, and their cells began to differentiate into stigmatic papillae (Fig. 4). In the ovary, ovules could be seen as round bulges emerging from the placentae (Fig. 5). By the end of phase D, the bud was 13 d old, about halfway through its development.

Phase E (stages 9–10)

The beginning of stage 9 was marked by the formation of a ventral furrow at the junction between the corolla tube and

Fig. 2. Stages of *Antirrhinum* flower development. Stage 0–1. Top-view scanning electron micrograph (SEM) of an inflorescence apex, including the first 8 plastochrons (labeled P0–P7). Stage 1 begins at plastochron 6, where the floral meristem (f) can be observed. The bract primordium has been removed from plastochron 7 and all subsequent plastochrons. For stages 2–11, an SEM of a representative plastochron from each stage of flower development was selected and shown with the dorsoventral axis running from top to bottom. From stage 5 onwards, the sepals of whorl 1 have been removed to reveal the inner floral whorls. For stages 2–14, a photograph of a representative plastochron from each stage was selected. Arrows indicate hair cells at stage 8, the ventral furrow at stage 9, hair cells on the ventral petal lobe at stage 10, and an anthocyanin pigment sector at stage 12. P, plastochron; f, floral meristem; ds, dorsal sepal; ls, lateral sepal; vs, ventral sepal; dp, dorsal petal; lp, lateral petal; vp, ventral petal; dst, dorsal staminode; lst, lateral stamen; vst, ventral stamen; c, carpel. Scale bars = 100 μm (stages 0–8) and 1 mm (stages 9–14).

Table 1. Summary of the phases of *Antirrhinum* flower development.

Phase	Age of flower at end of phase (d)	Stage	Plastochron	Meristem or bud width (mm)	Bud height (mm)	Morphology
A	3	0	0–5	0.04–0.15[a]		Bract emergence
		1	6–7	0.11–0.14[a]		Floral meristem emergence
B	7	2	8–11	0.14–0.16[a]		Loaf-shaped floral meristem
		3	12–13	0.16–0.24[a]		Fivefold floral symmetry
		4	14–17	0.24–0.3[a]		Sepal emergence
C	10	5	18–20	0.3–0.4		Petal + stamen emergence
		6	21–24	0.4–0.7		Carpel emergence
D	13.3	7	25–28	0.8–1.2		Microsporangia form on stamens
		8	29–32	1.3–1.7		Corolla covers internal whorls and hairs appear on the corolla tube. Stigmatic papillae develop. Ovule emergence.
E	16.7	9	33–36	1.8–2.3	1.5–1.9	Emergence of ventral furrow. Trichomes on abaxial surface of dorsal corolla lobes. Stigmatic lips part. Emergence of nucellus.
		10	37–40	2.5–3.3	2.0–3.0	Trichomes on abaxial surface of ventral corolla lobe. Anther sacs parallel to each other. Stigmatic lips come together. Emergence of funiculus.
F	20	11	41–44	3.5–4.0	3.5–5.0	Sepals stop growing. Cleft in ventral petal. Trichomes around the base of ventral stamen filaments.
		12	45–48	5.0–7.0	5.5–9.0	Anthocyanin pigmentation on corolla lobes. Elongation of stamens and style. Ovule appears mature.
G	24	13	49–52	7.0–12	10–20	Yellow pigmentation on adaxial corolla surface. Elongation of the corolla.
		14	53–57	15–24	22–40	Corolla unfolds and stops growing. Stamens become longer than style.

Note: For each phase the following data are summarized: the age in days; stage; plastochron number; meristem or bud size; and major morphological characteristics. From P18, the width of the bud was measured across the widest part of the corolla. Bud height is the distance from the base of the bud (excluding the pedicel) to its distal tip.

[a]Until the end of stage 4, the meristem width was calculated by measuring across the widest part of the whole floral meristem.

the lateral–ventral corolla lobes (arrow, Figs. 6 and 2). Trichome cells were visible on the abaxial surface of the dorsal corolla lobes (Fig. 2). The two locules on the adaxial surface of the anther sacs became more clearly defined at this stage (Fig. 3), and as whorl 4 developed, the stigmatic lips parted (Fig. 4). In the ovary, each ovule was a distinct outgrowth, and the more mature ovules in the centre of the placenta were pointed to one side where the nucellus was forming (arrow, Fig. 5, stage 9). By stage 10, the ventral furrow had deepened and hair cells had emerged on the abaxial surface of the ventral corolla lobe (Figs. 2 and 6). Cells on the adaxial surface of all corolla lobes began to adopt a more rounded shape. The anther sacs of the stamens curved down such that they were lying in parallel to each other (Fig. 3) and the stigmatic lips came together (Fig. 4). In the ovary, the nucellus of each ovule was now distinct (arrow, Fig. 5) and pointing downwards.

Phase F (stages 11–12)

During stage 11, the ventral furrow deepened as it grew inwards to form an indentation or cleft (Figs. 2 and 6). Trichome cells were visible around the base of the ventral stamen filaments (arrow, Fig. 3, stage 11) and on the abaxial surface of the ovary wall. The funiculus that attaches the ovule to the placenta was clearly visible and the integument almost covered the nucellus (Fig. 5). By the end of stage 11, the sepals of whorl 1 had reached their final dimensions.

During stage 12, anthocyanin pigmentation could first be detected as the corolla lobes emerged from the protective covering of the sepals. Figure 2 shows buds of *pal*^{rec}, which have sectors of pigment on an ivory background (arrow). The ventral furrow had deepened such that the ventral and lateral corolla lobes were folded back upon themselves, and the cells of the corolla had differentiated to define distinct regions such as the palate (distal part of the corolla tube) and

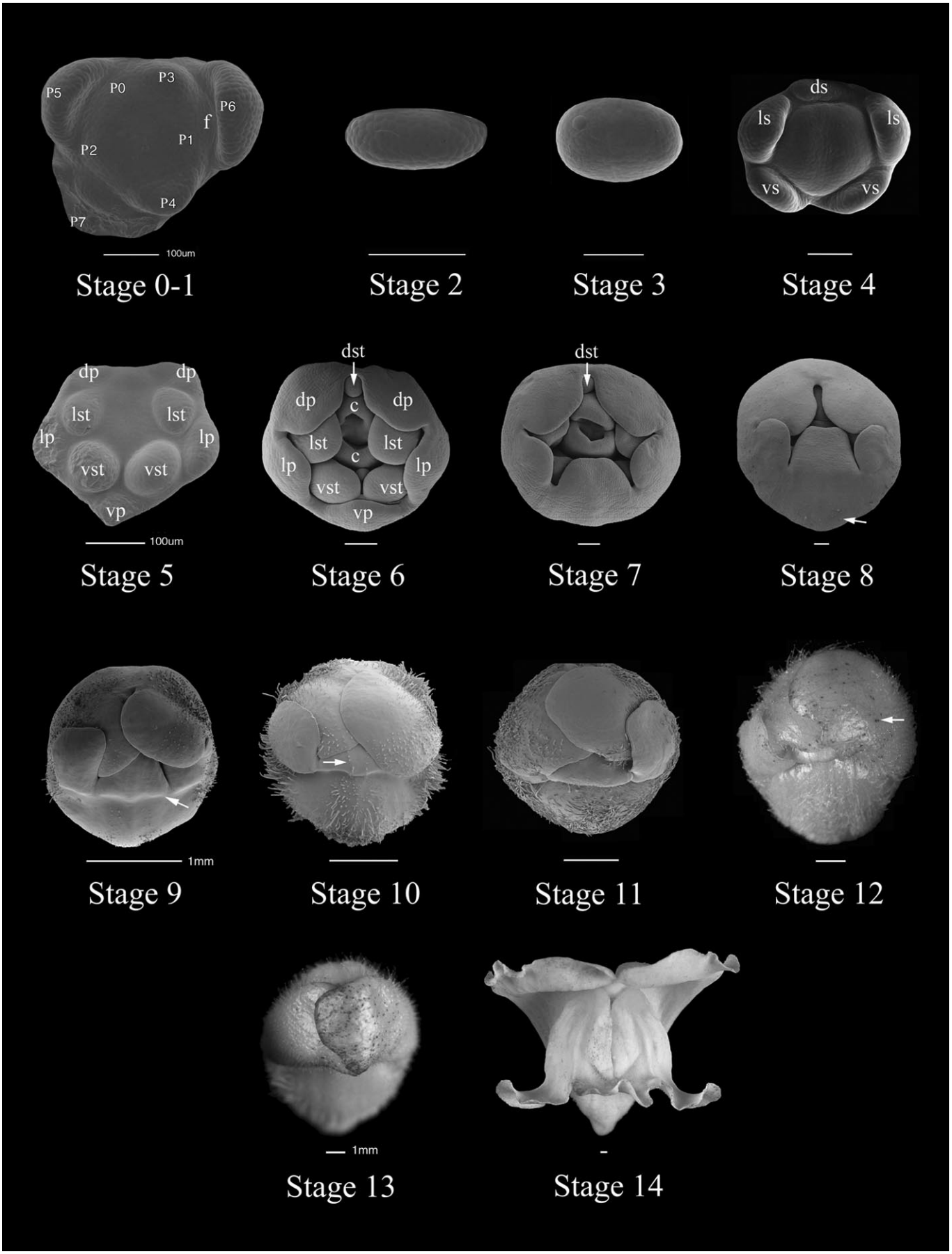

Fig. 3. Stamen development. Scanning electron micrographs of the adaxial side of developing ventral stamens for stages 8–12, and dissecting microscopy images of the front view of whorls 3 and 4 for stages 13 and 14. Arrow indicates trichomes around the base of the ventral stamens. loc, anther sac locules; fil, rudimentary filament; vst, ventral stamens; lst, lateral stamens. Scale bars = 200 µm (stage 8), 500 µm (stages 9–10), and 1 mm (stages 11–14).

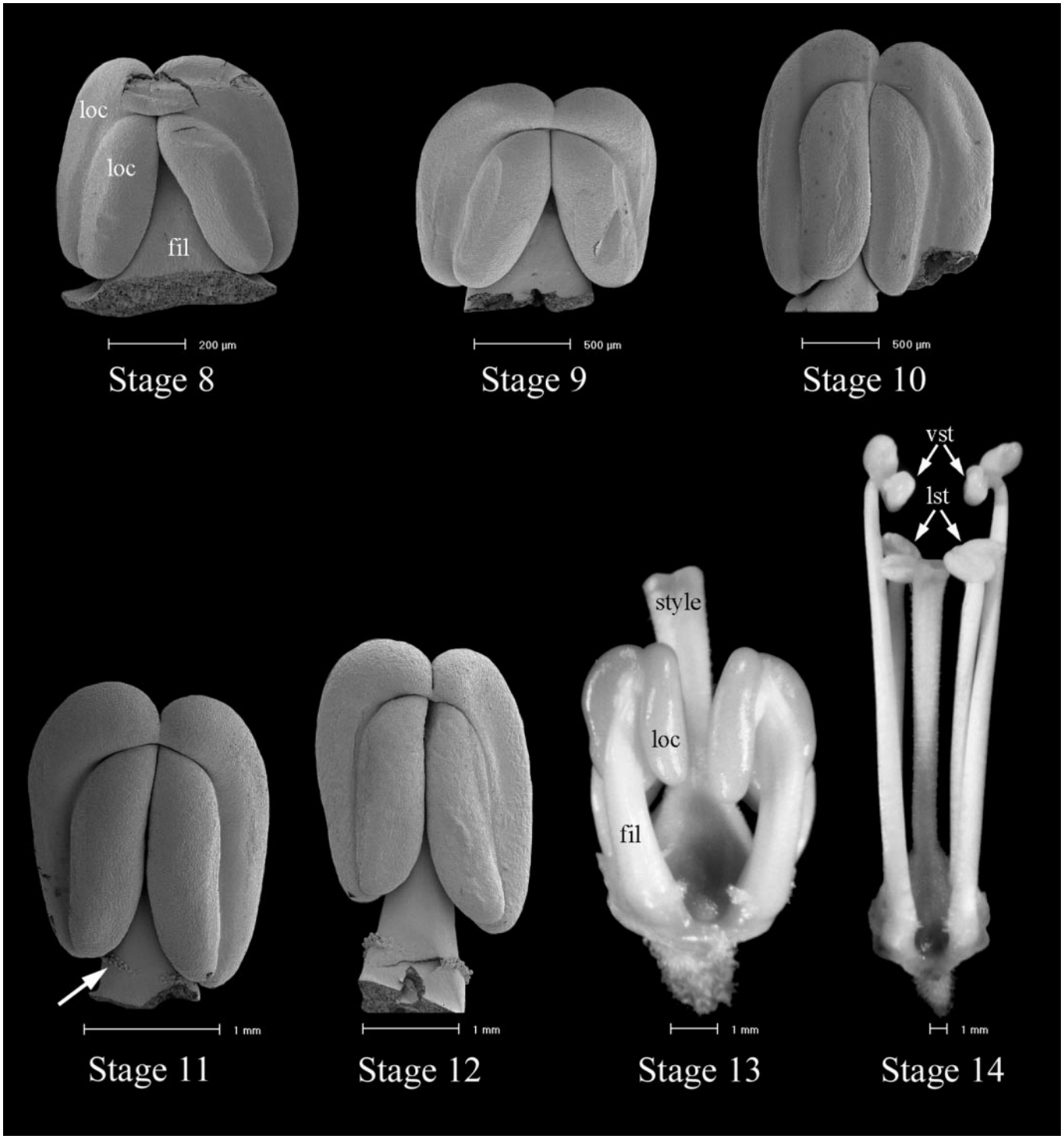

Fig. 4. Style development. Scanning electron micrographs of the stigmatic surface from stages 8 to 12. Dorsoventral axis of the flower runs from top to bottom in all SEMs. Trichomes on the ovary walls are indicated by an arrow in stage 12. sl, stigmatic lips. Scale bars = 200 μm (stages 8–11) and 500 μm (stage 12).

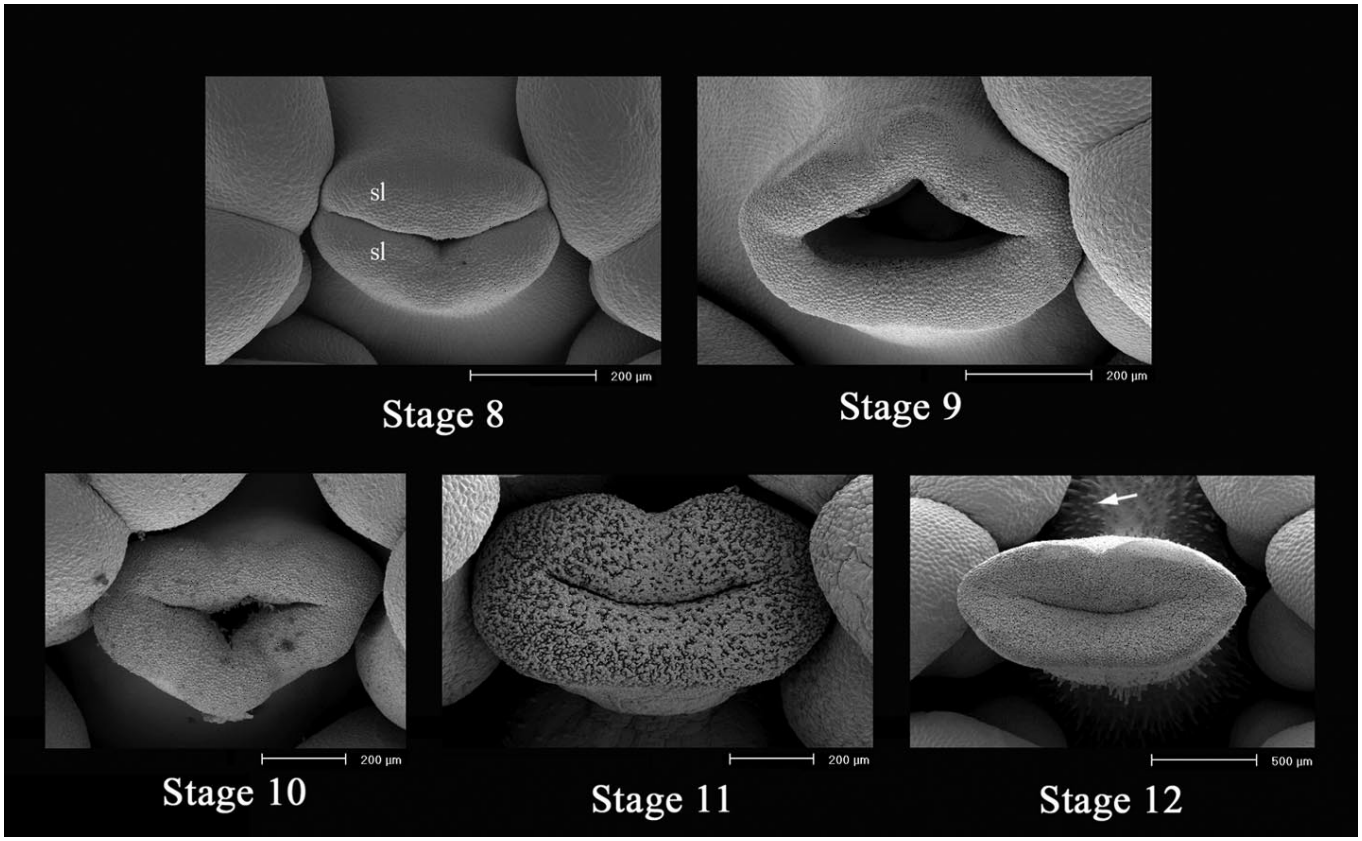

lip (proximal part of the corolla lobe) (Fig. 6). The anthers were raised by the stamen filaments, but were below the stigmas, which protruded from their centre (Fig. 3). Trichomes on the ovary wall were clearly visible (Fig. 4) and the integument covered the nucellus to form the micropylar opening (Fig. 5).

Phase G (stages 13–14)

During stage 13, yellow pigmentation around the trichomes on the adaxial surface of the corolla tube (throat region) was first detected. Although still tightly folded, the corolla had extended in height, giving the bud a more pointed appearance. The stamen filaments were now longer than the anther sacs, the two ventral stamens having elongated to a greater extent than the lateral ones (Fig. 3).

At stage 14, the corolla had expanded to its final dimensions and unfolded to give the flower its mature appearance (Fig. 2). The elongation of the stamen filaments continued until the mature ventral stamens were on average 23 mm long and the lateral ones were 18 mm long (Fig. 3). During this process of maturation and elongation, the stamens became twisted, so that their anther sacs were presented towards the ventral part of the flower, before they ruptured to release the mature pollen grains. Elongation of the style was surpassed by that of the lateral stamen filaments, so that in the mature flower, the style was shorter than the lateral stamens (Fig. 3).

Growth rates of sepals and petals

Aligned growth curves for the natural logarithm of the dorsal sepal and right dorsal petal areas are shown in Fig. 7A. The slope of these curves at any time indicates the specific growth rate in area at that time (Medawar 1945; see also legend to Fig. 7). For early stages (i.e., when ln(area) is less than 1), the specific rate of growth in area appeared constant and was similar for both petals and sepals. Linear regression showed that the specific growth rate in area per was 0.33 per plastochron (= 0.033 per h) for petals and 0.36 per plastochron (= 0.036 per h) for sepals. This corresponds to a doubling time in area of about 20 h (i.e., 2 plastochrons). At later stages (after ln(organ area) was more than 1), specific growth rate declined slightly in petals and much more for sepals. Sepal specific growth rate started to slow down after about P25 and ceased by about P45, while petals finished growing at about P57. Thus, it took about 31 plastochrons (13 d) for a sepal to grow (sepals first emerge at P14) and 39 plastochrons (16 d) for a petal to attain mature size (petals first emerge at P18).

Plots of bud width against plastochron number also indicated that the specific growth rate of width was constant early on (k = 0.14, Fig. 7B). Growth was maintained at a slightly lower rate after this until the mature flower width was attained, similar to the pattern observed with growth in petal area.

Fig. 5. Ovule development. Scanning electron micrographs of the placenta from stages 8 to 12. The carpel wall has been removed to reveal the placenta and developing ovules. The proximodistal axis of the flower runs from top to bottom in the top panel of SEMs. The bottom panel is orientated to reveal the micropylar opening. Arrows indicate an ovule primordium in stage 8, the nucellus in stages 9 and 10, and the micropylar opening in stage 12. i, integument; f, funiculus. Scale bars = 100 µm (stage 8) and 50 µm (stages 9–12).

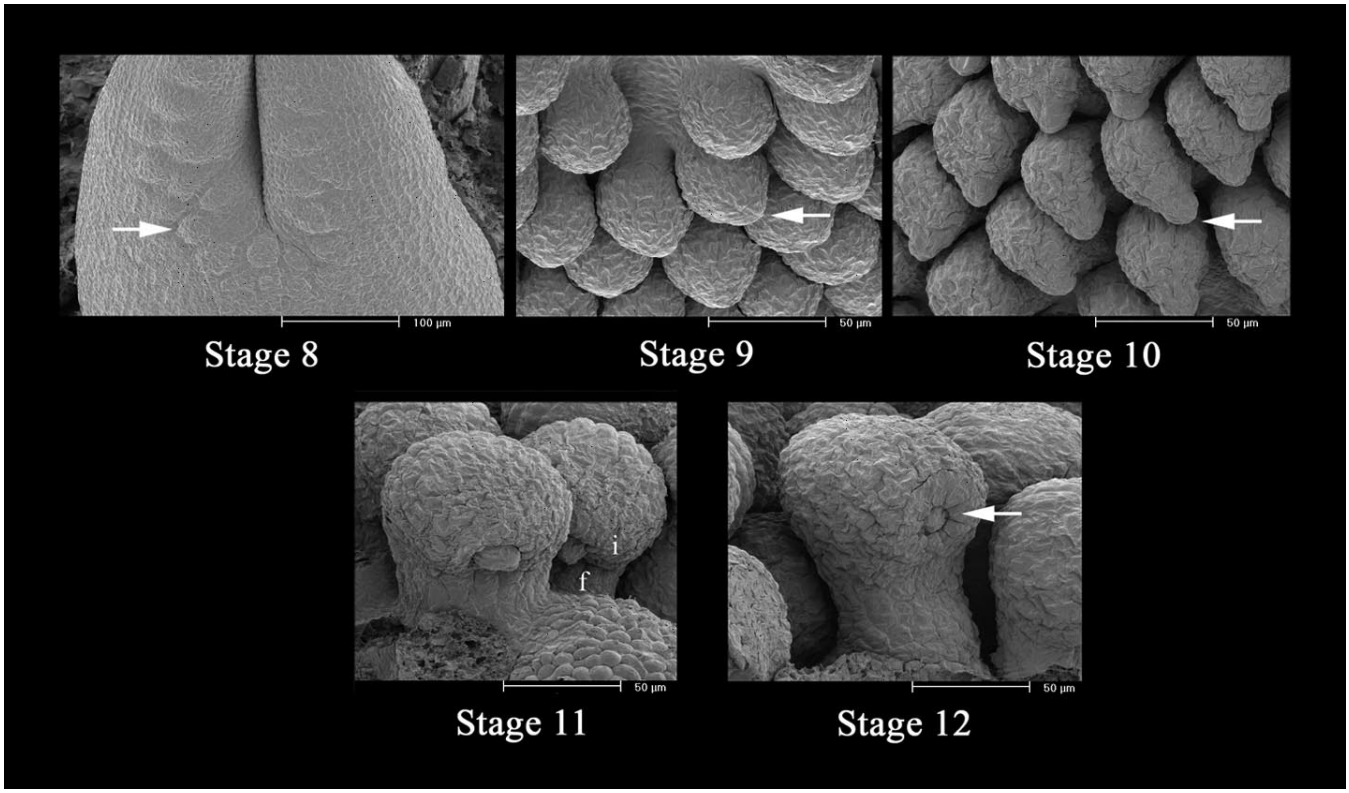

Fig. 6. Ventral furrow. Scanning electron micorgraphs of longitudinal sections of the ventral corolla at the lobe–tube boundary for stages 9–12. The proximodistal axis of the flower runs from bottom to top, and the arrow indicates the position of the ventral furrow in all stages. Scale bar = 200 µm.

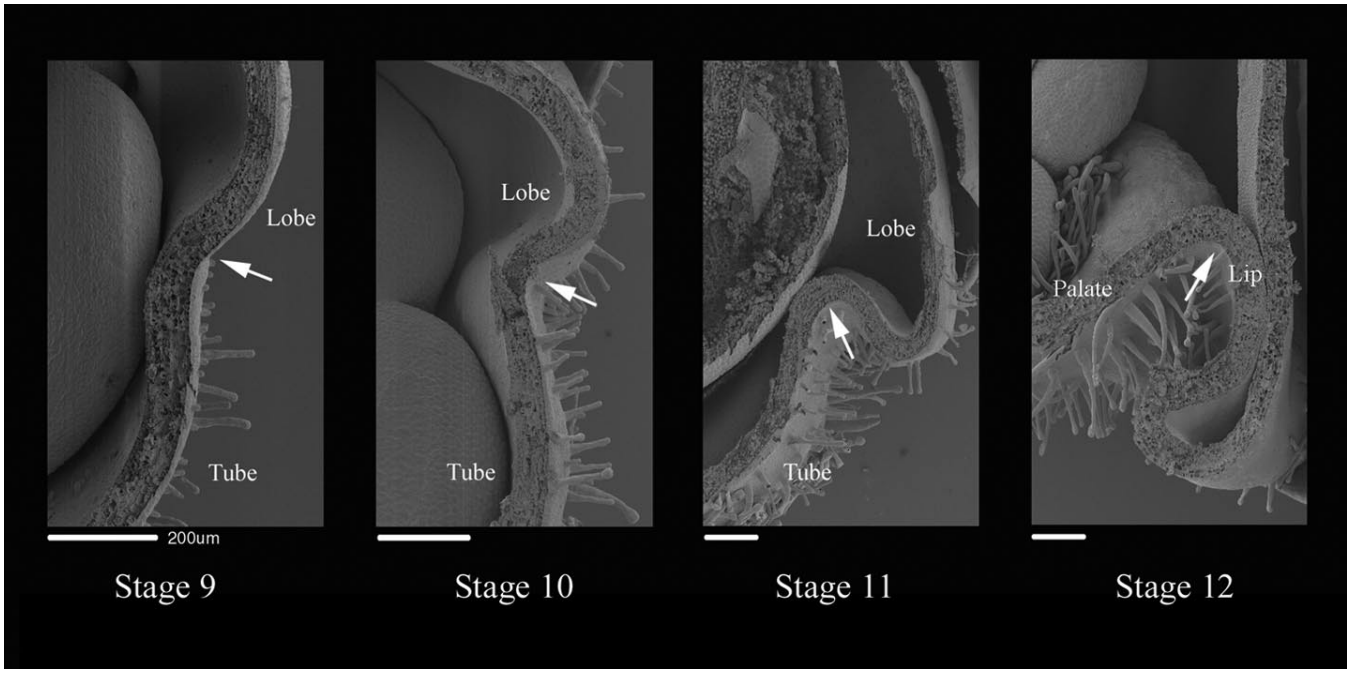

Fig. 7. (A) Sepal and petal growth curves. Natural logarithm of dorsal sepal or dorsal petal area (mm^2) against plastochron. Initially the specific growth rate for both organs is similar. The dorsal petal maintains this rate for most of its development, while growth of the dorsal sepal slows down gradually at later stages. For constant specific growth rate, the growth equation is given by $y = be^{kt}$ (Medawar 1945). The absolute rate of growth is the derivative of this, $dy/dt = kbe^{kt}$. The specific rate of growth is therefore $dy/y\,dt = k$. The value of k can be estimated from the slope of the logarithmic plot, as $\ln(y) = \ln(b) + kt$. Linear regression (lines shown in black) for values of ln(area) less than 1 gives $\ln(b) = -10.5$ and $k = 0.33$ per plastochron for petal area and $\ln(b) = -8.8$ and $k = 0.36$ per plastochron for sepal area. Average of sepal measurements are shown as squares, petal measurements as circles. Open symbols indicate points used for linear regression. (B) Flower width growth curves. Natural logarithm of flower width (mm), measured across the widest point of the corolla, plotted against plastochron. Linear regression (black lines) for ln(width) less than 1 gives values of $\ln(b) = -3.95$ and $k = 0.14$ per plastochron. Open circles indicate points used for linear regression.

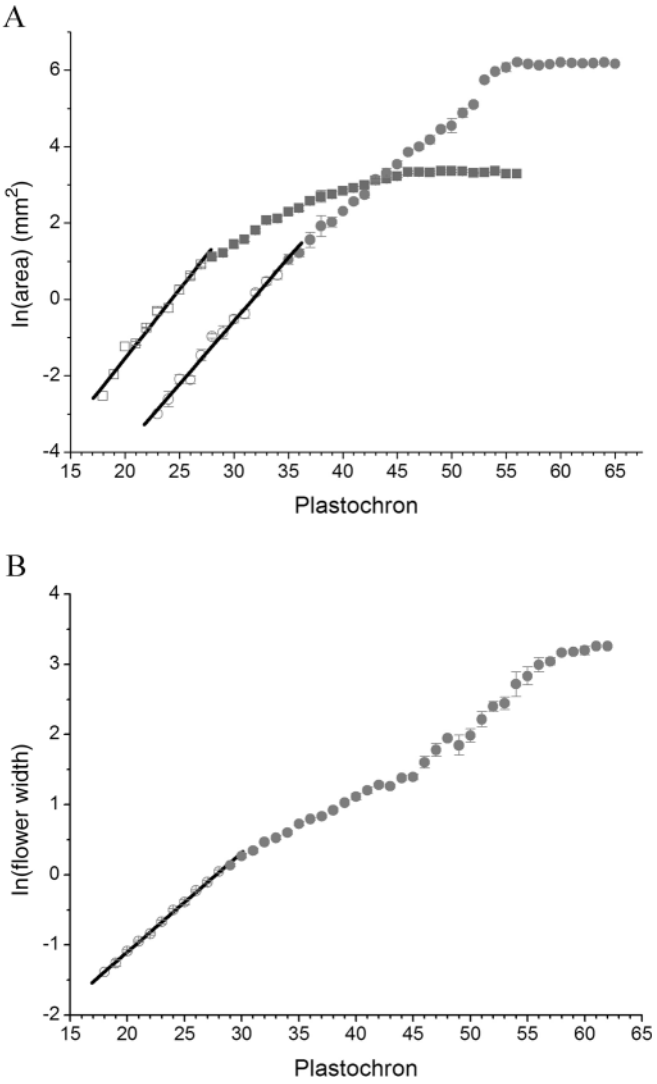

Discussion

We have determined the time course of *Antirrhinum* flower development from initiation to maturity. This has allowed growth rates and the timing of morphological transitions to be assessed. It is convenient to divide development into 15 stages, each lasting about 4 plastochrons, or 40 h under standard conditions. The stages can be further grouped into 7 phases, A–G, each lasting about 8 plastochrons.

During phase A, the floral meristem is initiated in the axil of a bract primordium on the flanks of the inflorescence apex and grows to form an elliptical mound of cells. This is the period when the floral meristem identity genes, such as *FLORICAULA* and *SQUAMOSA*, are first expressed (Coen et al. 1990; Huijser et al. 1992). In the next period, phase B, the meristem adopts five-fold symmetry and the first whorl of organs, the sepals, emerge. Organ identity genes, such as *DEFICIENS* and *PLENA*, are activated by the end of this phase (Bradley et al. 1993; Schwarz-Sommer et al. 1992). During phase C, the remaining three whorls, petals, stamens, and carpels, emerge in sequence. During phase D, the petal primordia grow to completely cover the inner whorls and ovules begin to emerge. In phase E, some cell types, such as hair cells, begin to differentiate and subregions of the organs start to acquire distinct features: the lower palate of the corolla starts to form and the anther sacs and ovules begin to adopt their characteristic morphologies. This process is completed during phase F. The last period, phase G, involves expansion and opening of the corolla and elongation of the stamens and stigma. As the earlier phases of growth have been described previously (Carpenter et al. 1995), here we concentrate on some of the later events that occur during phases D–G.

During these final four phases, petals grow at a relatively constant rate, doubling in area every 15–20 h. Estimates of cell sizes combined with clonal analysis indicates that growth during phases D–F is associated with cell division, while growth during phase G is largely a result of cell expansion (Rolland-Lagan et al. 2003). The near-constant growth rate through both cell division and expansion phases suggests there may be an overall control of petal growth rate independent of whether cell division is involved. Relatively uniform growth rates for bud lengths have also been described for other members of the Scrophulariaceae, although there can be variation in rates between genotypes (Kampny et al. 1994; Fenster et al. 1995).

Sepals initially grow during phase C at a similar rate to petals of a comparable size, even though sepal primordia are initiated earlier. However, sepal growth starts to slow down as buds enter phase D and stops during the middle of phase F. Thus, sepals are smaller than petals for two reasons: they grow for a shorter period (13 compared with 16 d) and their rate of growth declines at later stages. Sepals also grow more rapidly in length than in width, so that their shape becomes progressively more elongated during development.

A notable feature of *Antirrhinum* flower development is the formation of the lower palate and lips. We show that this involves the formation of an in-growing ventral furrow at the start of phase E, about halfway through flower development. The furrow lies at the tube–lobe boundary. Based on the sequence of scanning electron micrographs, the proximal side

of the furrow grows to form the lower palate, an extension of the tube. The distal side of the furrow grows to form the region of the lower lobes (the lips) that adjoin the palate. These regions are missing or reduced in *lipless* mutants, which also lack a clear ventral furrow (Keck et al. 2003). The formation and development of a ventral furrow has also been observed in other members of the Scrophulariaceae, such as *Digitalis lanata* (Ritterbusch and Wunderlin 1989).

The time course of *Antirrhinum* development can be compared with that of *Arabidopsis*, a distantly related model species with much smaller flowers. *Arabidopsis* plants grown in conditions similar to those employed here have a floral plastochron of about 12.5 h, as compared with 10 h for *Antirrhinum* (Smyth et al. 1990). Flower development in *Arabidopsis* has been staged according to morphology. Unlike *Antirrhinum*, there is no stage 0 corresponding to bract emergence in *Arabidopsis*, as flowers are not subtended by bracts. In *Arabidopsis* it takes about 15 d from the start of stage 1 to attain its final morphology (stage 14), as compared with 22 d in *Antirrhinum*. Thus, relative to *Antirrhinum*, *Arabidopsis* flowers cease growing and differentiate at a much earlier stage, correlating with their smaller size and shorter duration of development. Duration of growth has also been shown to play a major part in distinctions in corolla size between more closely related species, such as *Mimulus micranthus* and *Mimulus guttatus* (Fenster et al. 1995), and between cleistogamous and open forms of *Viola odorata* (Mayers and Lord 1984). It would be interesting to know whether the duration of certain stages of development are particularly amenable to modification during evolution.

Acknowledgements

The authors thank Stephen Impey for providing programs for area calculations, Desmond Bradley for helpful comments on the manuscript, and Rosemary Carpenter for providing plant material and advice.

References

Awasthi, D.K., Kumar, V., and Murty, Y.S. 1984. Flower development in *Antirrhinum majus* L. (Scrophulariaceae) with a comment upon corolla tube formation. Bot. Mag. Tokyo, **97**: 13–22.

Bradley, D., Carpenter, R., Sommer, H., Hartley, N., and Coen, E. 1993. Complementary floral homeotic phenotypes result from opposite orientations of a transposon at the *plena* locus of *Antirrhinum*. Cell, **72**: 85–95.

Canne-Hilliker, J.M. 1987. Patterns of floral development in *Agalinis* and allies (Scrophulariaceae). II. Floral development of *Agalinis densiflora*. Am. J. Bot. **74**: 1419–1430.

Carpenter, R., Martin, C., and Coen, E.S. 1987. Comparison of genetic behaviour of the transposable element Tam3 at two unlinked pigment loci in *Antirrhinum majus.* Mol. & Gen. Genet. **207**: 82–89.

Carpenter, R., Copsey, L., Vincent, C., Doyle, S., Magrath, R., and Coen, E. 1995. Control of flower development and phyllotaxy by meristem identify genes in *Antirrhinum*. Plant Cell, **7**: 2001–2011.

Coen, E.S., Romero, J.M., Doyle, S., Elliott, R., Murphy, G., and Carpenter, R. 1990. *floricaula*: a homeotic gene required for flower development in *Antirrhinum majus*. Cell, **63**: 1311–1322.

Endress, P.K. 1998. *Antirrhinum* and Asteridae — evolutionary changes of floral symmetry. Soc. Exp. Biol. Semin. Ser. **51**: 133–140.

Erickson, R.O., and Michelini, F.J. 1957. The plastochron index. Am. J. Bot. **44**: 297–305.

Fenster, C.B., Diggle, P.K., Barrett, S.C.H., and Ritland, K. 1995. The genetics of floral development differentiating two species of *Mimulus* (Scrophulariaceae). Heredity, **74**: 258–266.

Green, P.B., and Linstead, P. 1990. A procedure for SEM of complex shoot structures applied to the inflorescence of snapdragon (*Antirrrhinum*). Protoplasma, **158**: 33–38.

Huijser, P., Klein, J., Lonnig, W.E., Meijer, Saedler, H.H., and Sommer, H. 1992. Bracteomania, an inflorescence anomaly, is caused by the loss of function of the MADS-box gene *squamosa* in *Antirrhinum majus*. EMBO J. **11**: 1239–1250

Kampny, C.M. 1995. Pollination and flower diversity in Scrophulariaceae. Bot. Rev. **6**: 350–366.

Kampny, C.M., Dickinson, T.A., and Dengler, N.G. 1994. Quantitative floral development in *Pseudolysimachion* (Scrophulariaceae): intraspecific variation and comparison with *Veronica* and *Veronicastrum*. Am. J. Bot. **81**: 1343–1353.

Keck, E., McSteen, P., Carpenter, R., and Coen, E. 2003. Separation of genetic functions controlling organ identity in flowers. EMBO J. **22**: 1–9.

Lohmann, J.U., and Weigel, D. 2002. Building beauty: the genetic control of floral patterning. Dev. Cell, **2**: 135–142.

Mayers, A.M., and Lord, E.M. 1984. Comparative flower development in the cleistogamous species *Viola odorata*. III. Histological study. Bot. Gaz. **145**: 83–91.

Medawar, P.B. 1945. Size, shape and age. *In* Essays on growth and form. *Edited by* W.E. Le Gros Clark and P.B. Medawar. Clarendon Press,Oxford.

Reeves, P.A., and Olmstead, R.G. 1998. Evolution of novel morphological and reproductive traits in a clade containing *Antirrhinum majus* (Scrophulariacea). Am. J. Bot. **85**: 1047–1056.

Ritterbusch, A. 1990*a*. The construction of plastochron ordered sequences in flower ontogenesis. Flora, **184**: 313–323.

Ritterbusch, A. 1990*b.* The measure of biological age in plant modular systems. Acta Biotheor. **38**: 113–124.

Ritterbusch, A., and Wunderlin, U. 1989. On growth and development — a spatio-temporal analysis of flower ontogenesis. Environ. Exp. Bot. **29**: 111–121.

Rolland-Lagan, A.-G., Bangham, A., and Coen, E. 2003. Growth dynamics underlying petal shape and asymmetry in *Antirrhinum.* Nature (Lond.), **422**: 161–163.

Schwarz-Sommer, Z., Hue, I., Huijser, P., Flor, P.J., Hansen, R., Tetens, F., Lonnig, W.-E., Saedler, H., and Sommer, H. 1992. Characterization of the *Antirrhinum* floral homeotic MADS-box gene *deficiens*: evidence for DNA binding and autoregulation of its persistent expression throughout flower development. EMBO J. **11**: 251–263.

Singh, V., and Jain, D.K. 1979. Floral organogenesis in *Antirrhinum majus* (Scrophulariaceae). Proc. Indian Acad. Sci. Sect. B, **88**: 183–188.

Smyth, D.R., Bowman, J.L., and Meyerowitz, E.M. 1990. Early flower development in *Arabidopsis*. Plant Cell, **2**: 755–767.